Hydrogen-induced metallicity of $SrTiO_3$ (001) surfaces: A density functional theory study

Feng Lin, Shanying Wang, Fawei Zheng, Gang Zhou, Jian Wu, Bing-Lin Gu, and Wenhui Duan*
Department of Physics, Tsinghua University, Beijing 100084, People's Republic of China
(Received 14 August 2008; revised manuscript received 16 November 2008; published 13 January 2009)

The effect of atomic hydrogen adsorption on TiO_2-terminated and SrO-terminated $SrTiO_3$ (001) surfaces is studied using density functional theory calculations. Several adsorption coverages (1/12, 1/6, 1/3, 1/2, 2/3, and 1 monolayer) are considered. It is found that the hydrogen adsorption shows site selectivity and causes remarkable surface distortion. Surface metallicity induced by the hydrogen adsorption is observed and revealed to be caused by the electron donation from hydrogen to the surface. Our results suggest a mechanism of hydrogen-induced degradation and hydrogen-sensitive *I-V* characteristics of $SrTiO_3$-based devices.

DOI: 10.1103/PhysRevB.79.035311 PACS number(s): 73.20.At, 68.43.Bc, 73.20.Hb, 68.43.Fg

I. INTRODUCTION

In recent years, much attention has been paid to the effect of hydrogen on the properties of perovskite oxides.[1–5] As well known, perovskite oxides have been widely used as ceramic capacitors, variable resistors, and other electronic devices. The degradation induced by atomic hydrogen during forming gas annealing (FGA), however, limits the integration of perovskite oxides as nonvolatile memories in complementary metal oxide semiconductor based devices.[1,2] For example, it was experimentally observed that the leakage current density of $(Ba,Sr)TiO_3$ films increases with increasing annealing time in D_2/N_2 at 300 °C,[2] and the insulation resistance and capacitance of Pb-based perovskite oxide ferroelectrics are greatly decreased due to the atomic hydrogen generated by electrolysis of water.[6,7] Therefore, for the application of perovskite oxide devices, it is always of great importance to eliminate the degradation induced by hydrogen. On the other hand, hydrogen sensitivity of perovskite oxides can be taken advantage of for hydrogen sensor.[8] The metal-ferroelectric hydrogen sensor on an amorphous ferroelectric $(Ba_{0.67}Sr_{0.33})Ti_{1.02}O_3$ layer showed good hydrogen sensitivity of greater than 30 nA at the operating temperature range of 230–270 °C.[9]

One general mechanism of hydrogen-induced degradation and hydrogen-sensitive *I-V* characteristics of perovskite oxides devices is that hydrogen atoms diffuse into perovskite lattice as a shallow donor, resulting in a great increase in leakage currents. The electronic structure of hydrogen-doped bulk $SrTiO_3$ was theoretically studied by the DV-$X\alpha$ molecular-orbital method,[10] indeed showing hydrogen-induced shallow donor levels. On the other hand, the metallicity induced by adsorption of hydrogen atoms has been observed or predicted on semiconductor (such as SiC) surfaces[11,12] and metal oxide (such as ZnO) surfaces.[13,14] This suggests that the influence of hydrogen adsorption on perovskite oxide surfaces might be essential and significant since the hydrogen atoms generated by electrolysis of water should first be adsorbed on the perovskite oxide surfaces before they diffuse into the devices.[7] It is reasonable to expect that the adsorption of hydrogen atoms would also affect the electronic property of perovskite oxide surfaces. Such an effect may become more pronounced with the miniaturization of perovskite oxide devices down to the nanoscale, where the surface/bulk ratio of the devices increases greatly. So far, however, the theoretical studies about hydrogen adsorption on perovskite oxide surfaces have hardly been reported.

In this work, the adsorption of atomic hydrogen on TiO_2-terminated and SrO-terminated $SrTiO_3$ (001) surfaces is investigated using density functional theory (DFT), with a focus on the influence of hydrogen adsorption on the surface electronic structure. The dependence of hydrogen-adsorption states and the electronic properties on adsorption coverage is explored for both TiO_2-terminated and SrO-terminated surfaces with different adsorption coverages. From the analysis of band structure and charge transfer, the mechanism of hydrogen-adsorption-induced metallicity is revealed, which is useful for understanding hydrogen-induced degradation and hydrogen-sensitive *I-V* characteristics of perovskite oxide based devices (especially at nanoscale).

II. METHOD AND MODEL

All calculations are performed using the Vienna *ab initio* Simulation Package (VASP) (Ref. 15) based on the DFT, with the projector augmented-wave (PAW) method[16,17] and gradient-corrected exchange-correlation functional of Perdew and Wang (PW91).[18] In the calculations, 2*s* and 2*p* states are treated as valence states for O atom; 3*d* and 4*s* states are treated as valence states for Ti; and 4*s*, 4*p*, and 5*s* states are treated as valence states for Sr. And a plane-wave energy cutoff of 400 eV is used. The $SrTiO_3$ (001) surface is modeled using a periodic slab with a mirror symmetry,[19,20] which includes seven alternating TiO_2 and SrO layers, and the slabs are separated by a vacuum layer of 11 Å, as shown in Fig. 1. For the TiO_2-terminated surface, we consider five different adsorption coverages of 1/12, 1/6, 1/3, 2/3, and 1 ML (monolayer); for the SrO-terminated surface, we consider two different adsorption coverages of 1/2 and 1 ML. The 1×1 and 2×2 surface supercells are, respectively, chosen for higher adsorption coverages (1/3, 2/3, and 1 ML for the TiO_2-terminated surface and 1/2 and 1 ML for the SrO-terminated surface) and lower adsorption coverages (1/12, 1/6, and 1/3 ML for the TiO_2-terminated surface). Herein the atoms of the middle layer are fixed to simulate the bulk structure and the rest atoms are fully relaxed until the force is less than 0.01 eV/Å. The $15\times15\times1$ (for 1×1 surface su-

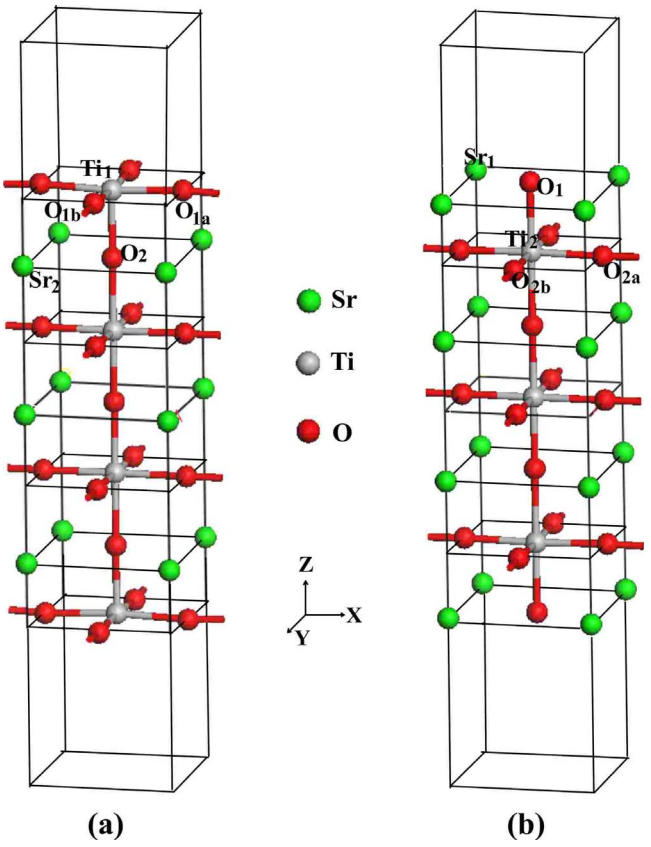

FIG. 1. (Color online) The 1×1 supercells of the slab model with (a) TiO_2-terminated surface and (b) SrO-terminated surface. In (a), Ti_1, O_{1a}, and O_{1b} (Sr_2 and O_2) represent the Ti and O atoms of the surface layer (the Sr and O atoms of the subsurface layer), respectively. In (b), Sr_1 and O_1 (Ti_2, O_{2a}, and O_{2b}) represent the Sr and O atoms of the surface layer (the Ti and O atoms of the subsurface layer), respectively. Green, gray, and red balls represent Sr, Ti, and O atoms, respectively.

percell) and $7\times7\times1$ (for 2×2 surface supercell) Monkhorst-Pack k-point meshes are used in the Brillouin-zone integration.

To examine the above calculation parameters, we calculate the structural properties of $SrTiO_3$ bulk and clean surfaces. The calculated bulk lattice constant is 3.945 Å, consistent with the experimental value (3.905 Å) and the previous theoretical results.[21–25] The $SrTiO_3$ (001) surface structure is characterized by the amplitudes of surface rumpling s (the relative displacement of oxygen with respect to the metal atom in the surface layer) and the changes in interlayer distances Δd_{ij} (i and j are the numbers of the layers). As shown in Table I, our results agree very well with all previous theoretical studies,[22,23,25] but there exists a discrepancy between theoretical and experimental results.[26,27] It should be noted that even the data of Δd_{ij} are not consistent between different experiments.[26,27]

III. RESULTS AND DISCUSSION

A. Optimized structures and adsorption energies

Figure 2(a) shows the optimized structure of the TiO_2-terminated $SrTiO_3$ surface with the coverage of 1/3 ML, where only one hydrogen atom is adsorbed on the 1×1 surface supercell. It is found that the hydrogen atom does not bond with the surface Ti atom but is adsorbed near the O atom, as seen from Fig. 2(a). In detail, the hydrogen atom ($H_{O_{1a}}$) bonds with the surface O atom (O_{1a}) and pulls it out of the surface by about 0.57 Å. Similar surface distortion caused by hydrogen adsorption was also observed on the ZnO $(10\bar{1}0)$ surface, where the adsorbed hydrogen atoms pull the surface Zn and O atoms of the ZnO surface out by 0.53 and 0.25 Å, respectively.[28] Such considerable surface distortion is an obvious consequence of the formation of the strong bond between H and O. The length of the O_{1a}-$H_{O_{1a}}$ bond is 0.984 Å, a little longer than that of the free OH^- (0.97 Å). Moreover, $H_{O_{1a}}$ also forms one weak O_{1a}-$H_{O_{1a}}$ bond with the O_{1a} atom in the neighboring supercell. This bond has a length of 3.00 Å in the range of weak hydrogen bonds (2.20–3.20 Å) and makes a small angle with the surface. The calculated adsorption energy of $H_{O_{1a}}$ is 1.64 eV, indicating predominant chemisorption. Herein the adsorption energy E_{ad} is defined as $E_{ad}=(E_{clean}+2E_H-E_{tot})/2$, where E_{clean}, E_{tot}, and E_H are the total energies of the clean surface, hydrogen-adsorbed surface, and a free hydrogen atom, respectively.

A higher adsorption coverage of 2/3 ML is obtained when one more hydrogen atom is adsorbed on the surface. Several initial adsorption configurations are carefully selected for structural optimization. We find two energetically stable ad-

TABLE I. Surface rumpling s and relative displacements Δd_{ij} (in percent of lattice constant) of the three near-surface planes of TiO_2-terminated and SrO-terminated $SrTiO_3$ (001) surfaces. Comparisons with previous theoretical (T) and experimental (E) results are given.

	TiO_2 terminated			SrO terminated		
	s	Δd_{12}	Δd_{23}	s	Δd_{12}	Δd_{23}
This study	2.12	−5.77	3.24	5.88	−6.95	2.83
Ref. 22 (T)	1.8	−5.9	3.2	5.8	−6.9	2.4
Ref. 23 (T)	1.79	−6.4	4.7	7.65	−8.4	3.45
Ref. 25 (T)	2.12	−5.79	3.55	5.66	−6.58	1.75
Ref. 26 (E)	2.1 ± 2	1 ± 2	-1 ± 1	4.1 ± 2	-5 ± 1	2 ± 1
Ref. 27 (E)	2.6	1.8	1.3	4.6	2.6	1.3

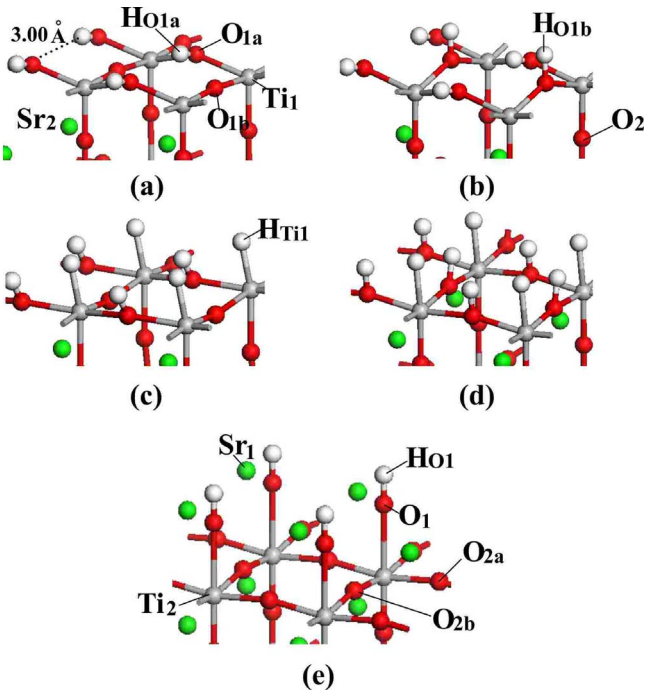

FIG. 2. (Color online) Optimized structures of hydrogen-adsorbed [(a)–(d)] TiO_2-terminated and (e) SrO-terminated $SrTiO_3$ surfaces, which are calculated using the 1×1 supercell. Four surface unit cells are shown here. (a), (d), and (e) correspond to the adsorption coverages of 1/3, 1, and 1/2 ML, respectively. (b) and (c) correspond to two different cases of 2/3 ML coverage, O-2/3 and Ti-2/3 ML. Green, gray, red, and white balls represent Sr, Ti, O, and H atoms, respectively.

sorption sites for the second hydrogen atom. One is near the second surface O (O_{1b}) site (the O-2/3 ML adsorption case) and the other is near the surface Ti (Ti_1) site (Ti-2/3 ML adsorption case), as shown in Fig. 2(b) and Fig. 2(c), respectively.

For the O-2/3 ML adsorption, the surface structure [see Fig. 2(b)] becomes more distorted. The surface O_{1a} and O_{1b} atoms are pulled out of the surface by about 0.710 and 0.824 Å, respectively. The O_{1b}-$H_{O_{1b}}$ bond is almost perpendicular to the surface, whereas the O_{1a}-$H_{O_{1a}}$ bond still makes a small angle with the surface. Both O_{1a}-$H_{O_{1a}}$ and O_{1b}-$H_{O_{1b}}$ bonds are about 0.985 Å long. The additional adsorption energy of the second hydrogen atom $H_{O_{1b}}$ is 0.61 eV. Herein, the additional adsorption energy is defined as $E_{ad}^{a}=(E_1+2E_H-E_2)/2$, where E_1, E_2, and E_H are, respectively, the total energies of 1/3 ML adsorption case, 2/3 ML adsorption case, and a free hydrogen atom. For the Ti-2/3 ML adsorption, the distortion of the surface structure [see Fig. 2(c)] is comparatively small. The surface Ti_1 and O_{1a} atoms are pulled out of the surface by only 0.150 and 0.263 Å, respectively. The length of the Ti_1-H_{Ti_1} bond is 1.748 Å, which is much longer than that of the O_{1a}-$H_{O_{1a}}$ bond (0.987 Å). Both Ti_1-H_{Ti_1} and O_{1a}-$H_{O_{1a}}$ bonds make apparent angles with the surface, about 75° and 62°, respectively. In this case, the additional adsorption energy of the second hydrogen atom H_{Ti_1} is 1.96 eV, about 1.35 eV larger than that of the O-2/3 ML adsorption case, which indicates that the Ti-2/3 ML adsorption is energetically more stable than the O-2/3 ML adsorption.

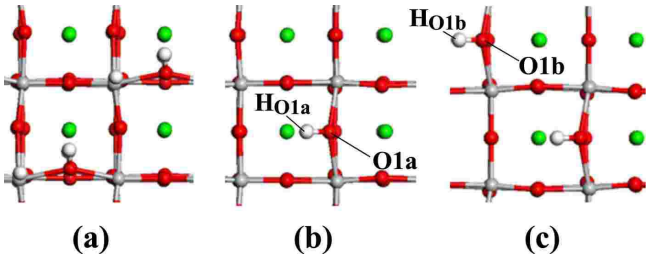

FIG. 3. (Color online) Top view of the optimized structures of hydrogen-adsorbed TiO_2-terminated $SrTiO_3$ surfaces, which are calculated using the 2×2 supercell. (a), (b), and (c) correspond to the adsorption coverages of 1/3, 1/12, and 1/6 ML, respectively. Note that there exist several different adsorption configurations for 1/3 and 1/6 ML coverages, while only the most energetically favorable ones are given here. Green, gray, red, and white balls represent Sr, Ti, O, and H atoms, respectively.

On the basis of the Ti-2/3 ML adsorption, the third hydrogen atom is introduced on the surface, resulting in a coverage of 1 ML [Fig. 2(d)]. It is found that the third hydrogen can be adsorbed stably near the surface O_{1b} site, as shown in Fig. 2(d). The surface distortion is also small. Ti_1, O_{1a}, and O_{1b} atoms are pulled out of the surface by 0.128, 0.277, and 0.211 Å, respectively, and the lengths of the Ti_1-H_{Ti_1}, O_{1a}-$H_{O_{1a}}$, and O_{1b}-$H_{O_{1b}}$ bonds are 1.888, 0.993, and 1.014 Å, respectively. The additional adsorption energy of the third hydrogen atom $H_{O_{1b}}$ is 1.79 eV, showing that the adsorption structure is rather stable.

It is notable that the additional hydrogen-adsorption energy of the Ti-2/3 ML adsorption (1.96 eV) is larger than the adsorption energy in the 1/3 ML adsorption (1.64 eV per H atom), which are all calculated in the 1×1 supercell. This suggests that for the coverage of 1/3 ML, an island adsorption of hydrogen might be energetically more favorable than a homogeneous adsorption [i.e., H atoms are all adsorbed on the surface O atoms, as shown in Fig. 2(a)].

To clarify this issue in detail, we have further studied the adsorption in a larger 2×2 surface supercell and explored the relative stability of different configurations in different adsorption coverages (1/3, 1/6, and 1/12 ML). Figure 3(a) shows the most energetically favorable configuration of the 1/3 ML adsorption where each two hydrogen atoms are adsorbed in the two adjacent O and Ti atoms and the calculated adsorption energy is 1.95 eV per H atom. Obviously, this adsorption mode ("pair adsorption") of 1/3 ML coverage is more favorable than the homogeneous adsorption.

Furthermore, we investigate hydrogen adsorption at lower coverages (1/12 and 1/6 ML). Figure 3(b) shows the 1/12 ML adsorption where one hydrogen atom ($H_{O_{1a}}$) is adsorbed on the O atom (O_{1a}) within the 2×2 supercell (i.e., four unit cells). The calculated adsorption energy of hydrogen is 2.26 eV per H atom, which is larger than the values at 1/3 ML and higher coverage. Figure 3(c) shows the most energetically favorable configuration of the 1/6 ML adsorption, with the adsorbed energy of 2.19 eV per H atom. It should be noted that in this case, both H atoms ($H_{O_{1a}}$ and $H_{O_{1b}}$) are adsorbed

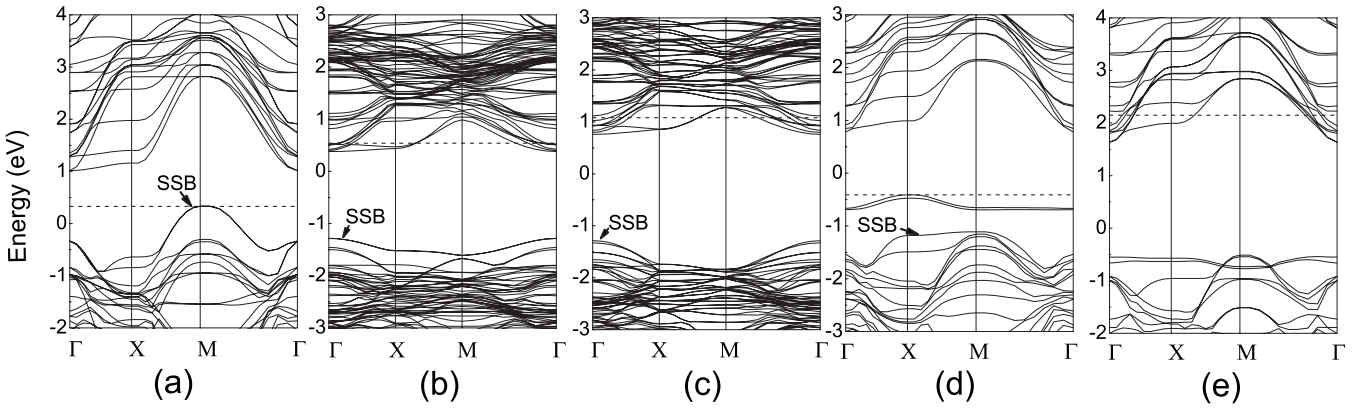

FIG. 4. Band structures of (a) clean and (b)–(e) hydrogen-adsorbed TiO_2-terminated $SrTiO_3$ surface. Herein, (b) and (c), respectively, correspond to the adsorption coverages of 1/12 and 1/6 ML, which are calculated using 2×2 supercell, while, (a), (d), and (e), respectively, correspond to the clean surface, Ti-2/3 ML adsorption, and 1 ML adsorption, which are calculated using 1×1 supercell. The Fermi level is denoted by the dashed line. Surface-state bands (SSBs) are denoted by arrows.

on two separated O atoms (O_{1a} and O_{1b}), and the pair adsorption is not energetically favorable any more.

The above results provide a clear picture of atomic hydrogen adsorption at TiO_2-terminated $SrTiO_3$ (001) surface. At low coverage, all H atoms prefer to adsorb on separated O atoms. With increasing hydrogen coverage, hydrogen atoms begin to adsorb on surface Ti atoms neighboring the O atom with adsorbed H atom, corresponding to pair adsorption. When all surface Ti atoms are consumed, hydrogen atoms continue to adsorb on remaining surface O atoms, finally leading to complete coverage.

Now we turn to the case of the SrO-terminated surface. The structure optimizations show that one hydrogen atom per surface unit cell can be adsorbed near the surface O atom [see Fig. 2(e)], corresponding to a coverage of 1/2 ML. The calculated adsorption energy is 2.06 eV. The formed O_1-H_{O_1} bond keeps perpendicular to the surface and the surface O atom moves out of the surface plane by about 0.43 Å. The length of the O_1-H_{O_1} bond is 0.977 Å. Interestingly, different from the case of the TiO_2-terminated surface, structural relaxation shows that two hydrogen atoms cannot be simultaneously adsorbed on one surface unit cell of the SrO-terminated surface. This means that the 1 ML adsorption coverage is not stable on the SrO-terminated $SrTiO_3$ (001) surface.

It is also important to check if a direct migration of H into the bulk is possibly preferred compared to an adsorption at the surface. We have calculated the binding energy of one H atom interstitially doped in bulk $SrTiO_3$ using a $2\times2\times2$ supercell. The obtained energy is 1.26 eV, which is smaller than the adsorption energies of H atom at both TiO_2-terminated and SrO-terminated $SrTiO_3$ (001) surfaces. This indicates that a direct migration of H into the bulk would not occur if the thermodynamic effects are not considered.

B. Electronic structures and hydrogen-induced metallicity

We first revisit the band structure of the clean TiO_2-terminated $SrTiO_3$ surface [see Fig. 4(a)]. The top of the valence bands is at the *M* point of the Brillouin zone. The two highest valence bands, which are degenerate at the *M* point, mainly come from the $2p$ orbitals of the surface O atoms and can be viewed as typical SSBs. The bottom of the lowest conduction band is located at the Γ point. The conduction bands near the Fermi level are predominantly contributed by the Ti atoms.

Then we discuss the effect of hydrogen adsorption on TiO_2-terminated $SrTiO_3$ surface. The band structure of the system with the 1/12 ML adsorption coverage is presented in Fig. 4(b). The most important characteristic is that the Fermi level shifts upward into the original conduction-band region with respect to that of the clean surface. The lower conduction bands are partially occupied, and consequently the surface becomes metallic. Another noticeable characteristic is that one of the SSBs of the clean surface disappears. This is mainly because the $H_{O_{1a}}$ $1s$ orbital strongly hybridizes with O_{1a} $2p$ and the resulting occupied hybrid band is significantly shifted down in energy (not shown in the figure). Similar disappearance of the SSBs upon hydrogen adsorption is widely observed in the semiconductor surfaces such as SiC (Ref. 12) and ZnO (Ref. 14) surfaces. The other SSBs, which arise predominantly from the $2p$ orbital of other surface O atoms, still remain after the adsorption but the dispersion is remarkably changed [see Fig. 4(b)]. Additionally, the lower conduction bands change significantly upon adsorption. This mainly results from the distortion of the surface structure, which is confirmed by calculating the band structure of the distorted surface with hydrogen atoms removed.

Figure 5(a) shows the charge redistribution of the system upon adsorption (with the coverage of 1/12 ML). We can see a depletion and an accumulation of electrons around the hydrogen atom ($H_{O_{1a}}$) and the surface Ti atom (Ti_1), respectively. Such charge transfer is very interesting since the H atom is adsorbed on the surface O atom instead of the Ti atom. It can be explained by a donation–back-donation mechanism.[14] The surface O atoms gain electrons from the adsorbed H atoms, and successively the neighboring metal atoms will gain electrons through the back donation from O atoms. As discussed above, the lower conduction bands

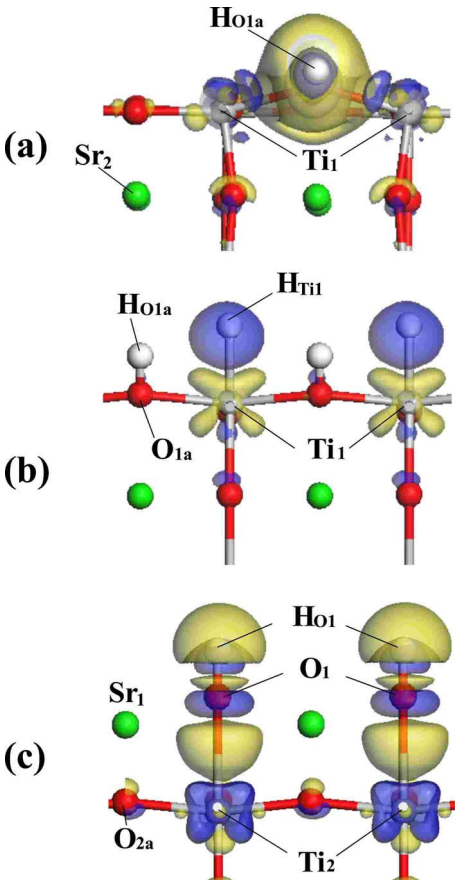

FIG. 5. (Color online) Electron density differences (side view) between (a) the TiO_2-terminated $SrTiO_3$ surface with the 1/12 ML hydrogen adsorption and the clean TiO_2-terminated surface plus individual H atoms, (b) the TiO_2-terminated surface with the Ti-2/3 ML hydrogen adsorption and that with the 1/3 ML coverage plus individual H atoms, and (c) the SrO-terminated $SrTiO_3$ surface with the 1/2 ML hydrogen adsorption and the clean SrO-terminated surface plus individual H atoms. The isosurfaces at the values of $0.06e/Å^3$ and $-0.06e/Å^3$ are depicted by the blue and yellow contours, respectively. Green, gray, red, and white balls represent Sr, Ti, O, and H atoms, respectively.

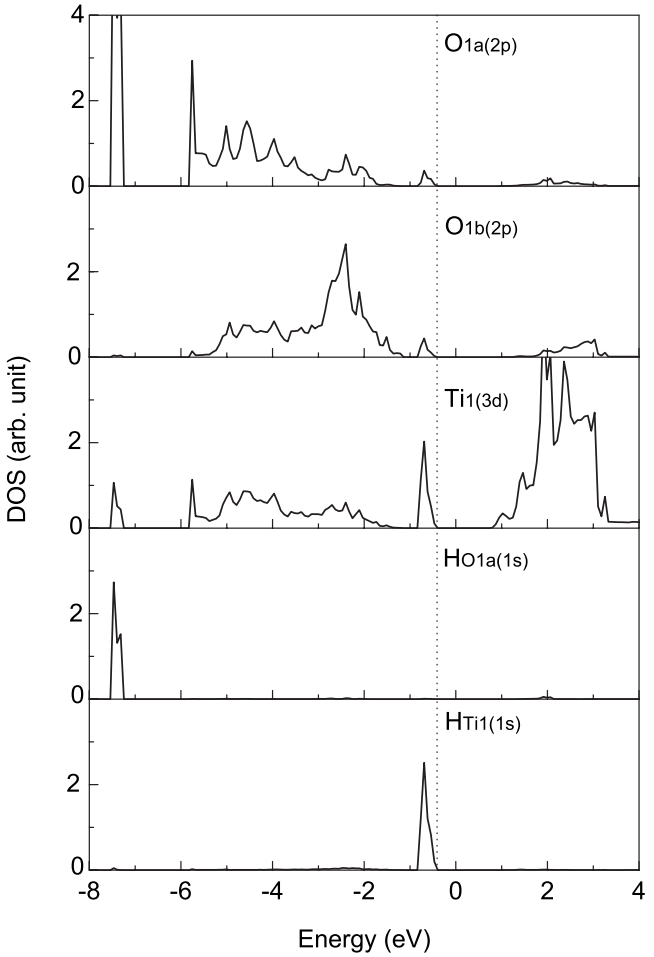

FIG. 6. APDOS of the TiO_2-terminated $SrTiO_3$ surface with the Ti-2/3 ML hydrogen adsorption. The Fermi level is denoted by the dashed line.

mainly come from the Ti atom. The electron transfer from H to Ti atom results in the upward shift of the Fermi level and the partially occupied conduction bands.

Surface metallicity is also observed in the 1/6 ML adsorption case [see Fig. 4(c)], which can be regarded as adsorbing an additional H atom ($H_{O_{1a}}$) around the O_{1b} atom of the 1/12 ML adsorption case [see Figs. 3(b) and 3(c)]. The second hydrogen provides electrons to the lower conduction bands, which are still partially occupied. The two H atoms, which are adsorbed separately near the two surface O atoms, cause a more pronounced surface structural distortion. As a result, the band structures are significantly changed as compared with those of the clean surface.

The situation is totally different when the second hydrogen atom is adsorbed near the surface Ti atom, forming the pair adsorption [e.g., the Ti-2/3 ML adsorption shown in Fig. 2(c)]. As shown in Fig. 4(d), the surface does not exhibit metallicity in this case. It is notable that two narrow hybrid bands with Ti_1 $3d$-H_{Ti_1} $1s$ character appear right below the Fermi level. Figure 6 shows the calculated atom-projected density of states (APDOS) of the system. The very sharp peaks just below the Fermi level, corresponding to the two narrow bands in Fig. 4(d), are mostly contributed by the Ti_1 and H_{Ti_1} atoms. Unlike $H_{O_{1a}}$, H_{Ti_1} does not donate electrons to the surface but gains electrons from the surface Ti atom, as shown in Figs. 5(a) and 5(b), forming a stronger H_{Ti_1}-Ti_1 bond. This is distinctly different from the case of the 1/12 ML adsorption coverage, where the adsorbed H atom cannot bond with the surface Ti atoms but only bond with O_{1a}. It can be understood by noting that the Ti_1 atom first gains electrons from the $H_{O_{1a}}$ (through back donation) and thus becomes more chemically active. As shown in Fig. 4(d), the SSB originating from the O_{1b} $2p$ still remains in the Ti-2/3 ML case. Moreover, the change in the band structure is comparatively small in this case since the structural distortion caused by hydrogen adsorption is small.

Figure 4(e) shows the band structure of the TiO_2-terminated $SrTiO_3$ surface with the adsorption coverage of 1 ML [Fig. 2(d)], which can be analyzed on the basis of the Ti-2/3 ML adsorption case. We can see that the remaining SSB is removed and the two narrow bands shift

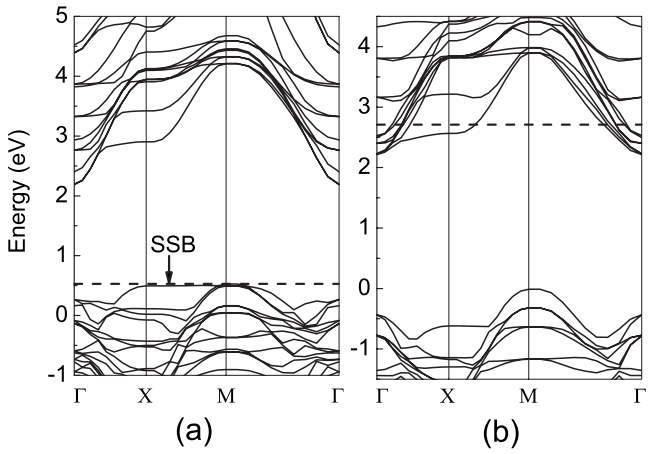

FIG. 7. Band structures of the (a) clean and (b) hydrogen-adsorbed (1/2 ML coverage) SrO-terminated $SrTiO_3$ surface. The Fermi level is denoted by the dashed line. SSB is denoted by the arrow.

down in energy and overlap with other upper valence bands. The fully saturated surface becomes metallic again because the third hydrogen atom ($H_{O_{1b}}$) donates extra electrons to the surface, and the Fermi level shifts up into the original conduction bands. This feature is interesting and different from what is observed in the ZnO surfaces where the surface metallicity appears only at low hydrogen coverage (1/2 ML) and disappears when the surface is fully saturated (1 ML coverage).[13,14]

Finally we discuss the effect of hydrogen adsorption on SrO-terminated $SrTiO_3$ surface. As shown in Fig. 7(a), the clean SrO-terminated surface has similar band characters near the Fermi level (except the SSB) as the clean TiO_2-terminated surface. The lower conduction bands mostly consist of the orbitals of the Ti atoms. The highest valence band that is very flat from *X* to *M* point is the SSB with surface O 2*p* character. For the 1/2 ML adsorption, the surface metallicity is observed [see Fig. 7(b)], which has the same physical mechanism as the 1/12 ML adsorption case of the TiO_2-terminated surface. Figure 5(c) displays a depletion and an accumulation of electrons around the hydrogen atom (H_{O_1}) and the subsurface Ti atom (Ti_2), respectively. Our structural optimization has shown that the 1 ML adsorption is unstable on the SrO-terminated surface. This can be understood from the band character of the $SrTiO_3$ surface. Actually, the Sr atoms make little contribution to the states near the Fermi level in both clean TiO_2-terminated surface and SrO-terminated surface. The chemically active states are those near the Fermi level such as the SSBs and Ti 3*d*. Hence the surface O and Ti atoms, instead of the surface Sr atoms, are the possible stable adsorption sites for hydrogen atoms.

IV. CONCLUSIONS

We have investigated the hydrogen adsorption and its effect on structural and electronic properties of $SrTiO_3$ (001) surface by DFT calculations. For TiO_2-terminated surface, H atoms prefer to adsorb on separated O atoms at low coverage. With increasing hydrogen coverage, hydrogen atoms begin to adsorb on surface Ti atoms adjacent to the O atom with adsorbed H atom. This adsorption mode, corresponding to pair adsorption, is energetically more favorable than the case that the two H atoms adsorb on the two adjacent O atoms. When all surface Ti atoms are consumed, hydrogen atoms continue to adsorb on rest surface O atoms, leading to full coverage finally. For the SrO-terminated surface, the structure optimization shows that the 1/2 ML adsorption coverage is stable but 1 ML adsorption coverage is not due to the chemical inactivity of the surface Sr atom. Generally, hydrogen adsorption can induce remarkable surface distortion.

It is found that TiO_2-terminated $SrTiO_3$ surface becomes metallic upon hydrogen adsorption in all cases except the pair adsorption cases (such as the Ti-2/3 ML). From the analysis of band structures and charge transfer, the mechanism of this metallicity induced by hydrogen adsorption revealed that the hydrogen atoms donate electrons to the surface, resulting in partial occupation of the lower conduction bands. This suggests that the hydrogen atoms generated by electrolysis of water can greatly influence the electronic properties of $SrTiO_3$-based devices even if they do not diffuse into the devices. In addition, we find that hydrogen atoms prefer to adsorb on the $SrTiO_3$ (001) surfaces rather than migrate into bulk if the thermodynamic effects are not considered. Our work reveals a unique mechanism of hydrogen-induced degradation and hydrogen-sensitive *I-V* characteristics of $SrTiO_3$-based devices. With the device miniaturization and increasing surface/bulk ratio of devices, such mechanism may play an important role in the device applications at nanoscale, where further experimental and theoretical studies about hydrogen adsorption on perovskite oxide surfaces are needed.

ACKNOWLEDGMENTS

This work was supported by the Ministry of Science and Technology of China (Grants No. 2006CB605105 and No. 2006CB0L0601) and the National Natural Science Foundation of China.

*Author to whom correspondence should be addressed.
dwh@phys.tsinghua.edu.cn

[1] S. Aggarwal, S. R. Perusse, C. W. Tipton, R. Ramesh, H. D. Drew, T. Venkatesan, D. B. Romero, V. B. Podobedov, and A. Weber, Appl. Phys. Lett. **73**, 1973 (1998).
[2] J. H. Ahn, P. C. McIntyre, L. W. Mirkarimi, S. R. Gilbert, J. Amano, and M. Schulberg, Appl. Phys. Lett. **77**, 1378 (2000).
[3] K. Xiong and J. Robertson, Appl. Phys. Lett. **85**, 2577 (2004); J.

S. Lee, Y. Li, Y. Lin, S. Y. Lee, and Q. X. Jia, *ibid.* **84**, 3825 (2004).
[4] M. Widerøe, R. Waser, and T. Norby, Solid State Ionics **177**, 1469 (2006); S. M. Wang and S. J. L. Kang, Appl. Phys. Lett. **89**, 041910 (2006).
[5] P. G. Sundell, M. E. Bjorketun, and G. Wahnstrom, Phys. Rev. B **76**, 094301 (2007); Y. Iwazaki, K. Morito, T. Suzuki, H. Kishi, and S. Tsuneyuki, Ferroelectrics **355**, 108 (2007).
[6] W. P. Chen, L. T. Li, Y. Wang, and Z. L. Gui, J. Mater. Res. **13**, 1110 (1998).
[7] W. P. Chen, H. L. W. Chan, F. C. H. Yiu, K. M. W. Ng, and P. C. K. Liu, Appl. Phys. Lett. **80**, 3587 (2002).
[8] W. Zhu, X. F. Chen, O. K. Tan, and J. Deng, Integr. Ferroelectr. **44**, 25 (2002).
[9] O. K. Tan, W. G. Zhu, M. S. Tse, and X. Yao, Mater. Sci. Eng., B **58**, 221 (1999).
[10] H. Yukawa, K. Nakatsuka, and M. Morinaga, Solid State Ionics **116**, 89 (1999).
[11] V. Derycke, P. G. Soukiassian, F. Amy, Y. J. Chabal, M. D. D'angelo, H. B. Enriquez, and M. G. Silly, Nature Mater. **2**, 253 (2003).
[12] H. Chang, J. Wu, B. L. Gu, F. Liu, and W. H. Duan, Phys. Rev. Lett. **95**, 196803 (2005).
[13] Y. Wang, B. Meyer, X. Yin, M. Kunat, D. Langenberg, F. Traeger, A. Birkner, and Ch. Woll, Phys. Rev. Lett. **95**, 266104 (2005).
[14] C. C. Wang, G. Zhou, J. Li, B. H. Yan, and W. H. Duan, Phys. Rev. B **77**, 245303 (2008).
[15] G. Kresse and J. Hafner, Phys. Rev. B **47**, 558 (1993).
[16] P. E. Blöchl, Phys. Rev. B **50**, 17953 (1994).
[17] G. Kresse and D. Joubert, Phys. Rev. B **59**, 1758 (1999).
[18] J. P. Perdew and Y. Wang, Phys. Rev. B **45**, 13244 (1992).
[19] J. Padilla and D. Vanderbilt, Phys. Rev. B **56**, 1625 (1997).
[20] S. Kajita, T. Minato, H. S. Kato, M. Kawai, and T. Nakayama, J. Chem. Phys. **127**, 104709 (2007).
[21] Z. Q. Li, J. L. Zhu, C. Q. Wu, Z. Tang, and Y. Kawazoe, Phys. Rev. B **58**, 8075 (1998).
[22] J. Padilla and D. Vanderbilt, Surf. Sci. **418**, 64 (1998).
[23] C. Cheng, K. Kunc, and M. H. Lee, Phys. Rev. B **62**, 10409 (2000).
[24] W. Luo, W. H. Duan, S. G. Louie, and M. L. Cohen, Phys. Rev. B **70**, 214109 (2004).
[25] R. I. Eglitis and D. Vanderbilt, Phys. Rev. B **77**, 195408 (2008).
[26] N. Bickel, G. Schmidt, K. Heinz, and K. Muller, Phys. Rev. Lett. **62**, 2009 (1989).
[27] T. Hikita, T. Hanada, M. Kudo, and M. Kawai, Surf. Sci. **287-288**, 377 (1993).
[28] P. Zapol, J. B. Jaffe, and A. C. Hess, Surf. Sci. **422**, 1 (1999).